Journal of Sound and Vibration (1997) **205**(2), 185–203

TRANSIENT RESPONSES OF POLYMERS AND ELASTOMERS DEDUCED FROM HARMONIC RESPONSES

M. Soula, T. Vinh and Y. Chevalier

Rheology and Structure Group, *Institut Supérieur des Matériaux et de la Construction Mécanique* (*ISMCM*), 93407-*Saint-Ouen Cedex*, *France*

(*Received* 15 *July* 1996, *and in final form* 21 *February* 1997)

The problem of interrelations between viscoelastic time and frequency functions is revisited. The proposed methods do not use the intermediary functions which are extensively used in the rheology of solid materials. Integer linear differential operators or fractional derivatives for constitutive equations relating stress and strain are the two possibilities of choice. From experimental curves of complex moduli versus frequency, obtained over a large range of frequencies, closed form expressions of moduli are obtained. Inverse Fourier transformation gives rise to time exponential series or time hypergeometric series depending on the type of constitutive law adopted.

1. INTRODUCTION

The evaluation of creep and relaxation time functions of linear viscoelastic materials deduced from the experimental curves of complex modulus versus frequency constitutes a classical and important problem in rheology. Theoreticians and experimentalists during the past 50 years have proposed a great number of methods. The technical literature concerning the interrelations of viscoelastic functions is very abundant. One can mention, among others, many contributions of Ferry [1], Tschoegl [2], and Schwartz and Staverman [3].

It is beyond the scope of this paper to present a complete review of existing methods. Only their main features are mentioned.

In rheology the experimental harmonic responses (complex moduli or their inverse complex compliances) must be presented over a very large range of frequencies, often more than eight decades. Although linear classical models such as generalized Maxwell models or generalized Voigt models are presented in textbooks devoted to viscoelasticity [1, 2], to the authors' knowledge, no attempt has been made to find a realistic number of springs and dashpots in parallel or in series, and their coefficients. Consequently experimentalists renounce using such attempts. In 1967, one of the authors [4] presented numerical and graphical methods to evaluate poles and zeros of quotients of polynomials versus angular frequency from complex moduli curves. The method proposed remains valid and its main features will be outlined in what follows.

The usual way adopted by rheologists is to evaluate intermediary functions called retardation or relaxation spectra, defined as follows:

0022–460X/97/320185 + 19 $25.00/0/sv970979

$$r(t) = \int_0^\infty e^{-t/\tau} H(\tau)\, d(\ln \tau), \qquad f(t) = \int_0^\infty (1 - e^{-t/\tau}) L(\tau)\, d(\ln \tau). \tag{1, 2}$$

$r(t)$ and $f(t)$ are the relaxation and the creep functions of time t. The kernels in equations (1) and (2), $H(\tau)$ and $L(\tau)$ are the so-called retardation and relaxation spectra which allow generalization of a finite number N of Maxwell models to continuous spectra, with N going to infinity. The Naperian logarithm of the relaxation (or retardation) time τ is used to evaluate, in a convenient manner, a very large range of time variables.

Such intermediary functions are obtained from harmonic responses and require the calculation of derivatives of these last functions with respect to angular frequency ω. A great variety of approximate formulae have been proposed, in which derivatives of various orders are used, to evaluate $H(\tau)$ and $L(\tau)$ [1–3]. Some approximate direct formulae have been proposed in which intermediary viscoelastic spectra are not used [1, 5].

The difficulty that the specialists in numerical computations met in the early 1960s can be explained by the fact that convenient computers were not available, nor were numerical programs for computing special series and algorithms for fast Fourier transforms.

In the field of structural dynamics, during the past 20 years, new viscoelastic high damping materials have been introduced in the construction of mechanical structures, the dynamic responses of which have to be calculated by finite element methods. Appropriate constitutive equations of viscoelastic materials must be provided so as to predict the dynamic behaviour of the structure.

Fractional derivatives have given rise, during the past 15 years, to a great amount of research in the theoretical domain as well as in practical applications. This mathematical formulation is in complete agreement with microstructural molecular theory of polymers proposed in the 1950s by Rouse [6] and improved by Ferry [7]. Padovan [8] and Kennedy and Padovan [9] adopted such a method to express the constitutive equation of rubber and applied this to the calculation of dynamic responses of automobile tyres. Bagley and Torvik [10] have made important contributions and have presented thermodynamic considerations so as to obtain consistent values of fractional powers in the constitutive equation. Morgenthaler [11] examined the problem of computation of eigenvalue concerning structures incorporating viscoelastic material described by fractional derivatives, using a frequency dependent complex stiffness matrix.

Gibson *et al*. [12] used discrete inverse Fourier transformation and numerical integration to solve the problem presented above by frequency/time integration valid for a long time range. The difference between Gibson's work and that to be presented in what follows resides in the fact that the relaxation functions are obtained here in closed form expressions. Long or short time ranges can be considered as special cases deduced from general formulae.

Fractional derivatives indeed constitute the most convenient way to describe the behaviour of realistic viscoelastic materials over a very large frequency range with a restricted number of parameters.

Evidently, the problem of interest here is concerned with materials science, but it may also be of concern to dynamic engineering, in the three following respects.

(i) Calculations of the structural responses require knowledge of the dynamic mechanical characteristics of viscoelastic materials used in a structure.

(ii) Often, the dependencies of the complex moduli (i.e., Young's and shear) of the material on the frequency are evaluated by various dynamic methods. In the framework of rheology, the problem is to find, from those complex quantities, the relaxation (or creep) functions which are the kernels in the convolution integrals expressing the material responses.

(iii) Relaxation time functions are obtained by conventional methods in rheology by using excitation as constant strains applied as a step (Heaviside) function. The stress responses are valid for times exceeding one minute. Dynamic tests permit one to obtain the material response for a shorter time. For this purpose, transient responses are deduced from harmonic ones.

In the first part of this paper, graphical and numerical methods are presented. The graphical method permits one to evaluate poles and zeros of the quotient of two polynomials representing the complex modulus versus frequency. The numerical method enables one to evaluate the coefficients of closed form expressions for complex moduli by using fractional derivatives.

In the second part of the paper inversion techniques via the inverse Fourier transform to obtain closed form expressions for transient responses of viscoelastic materials are presented.

2. CLOSED FORM EXPRESSIONS FOR COMPLEX MODULI

2.1. ANALYTIC EXPRESSIONS

Differential operators are used to relate stress σ to strain ε:

$$P\sigma = Q\varepsilon, \qquad P = \sum_{k=0}^{N} a_k \frac{\mathrm{d}^k}{\mathrm{d}t^k} \quad \text{and} \quad Q = \sum_{l=0}^{M} b_l \frac{\mathrm{d}^l}{\mathrm{d}t^l}. \tag{3, 4}$$

Here P and Q are sums of operators. N and M are the degrees of the operators. For solid materials, by using asymptotic considerations in the frequency domain, it can be shown that the degrees N and M must be equal.

The practical problem is to evaluate the degree $N = M$ which determines the number of terms in the series (4) and the $2N + 2$ coefficients a_p and b_q in the differential equation (3). N must not be arbitrarily fixed in advance. It must take into account the features the complex modulus curve versus frequency.

If one takes the Fourier transform of each term in equation (3), one obtains

$$P(\omega)\sigma^*(\omega) = Q(\omega)\varepsilon^*(\omega). \tag{5}$$

$P(\omega)$ and $Q(\omega)$ are two polynomials in the angular frequency ω with the same degree N:

$$P(\omega) = \sum_{p=0}^{N} a_p(\mathrm{j}\omega)^p, \qquad Q(\omega) = \sum_{q=0}^{N} b_q(\mathrm{j}\omega)^q. \tag{6}$$

Substituting equations (6) into equation (5) yields an expression for the complex modulus as the quotient of two polynomials:

$$E^*(\mathrm{j}\omega) = \frac{\sigma^*(\omega)}{\varepsilon^*(\omega)} = \frac{Q(\mathrm{j}\omega)}{P(\mathrm{j}\omega)} = \sum_{q=0}^{N} b_q(\mathrm{j}\omega)^q \Big/ \sum_{p=0}^{N} a_p(\mathrm{j}\omega)^p. \tag{7}$$

Written in terms of its poles, $-p_{ii} = P_i$ and zeros, $-z_{ii} = z_i$, equation (7) is

$$E^*(\mathrm{j}\omega) = A \prod_{i=1}^{N} (\mathrm{j}\omega + z_{ii}) \Big/ \prod_{i=1}^{N} (\mathrm{j}\omega + p_{ii}), \tag{8}$$

where A is a constant. In the complex plane $p = \sigma + j\omega$, the poles and zeros are all real and negative. Due to the properties of viscoelastic materials, $E^*(\omega)$ is a monotonically increasing function of ω and must not possess any extrema (z_i, p_i real) because of stability considerations. They must be localized on the left half-plane P with $\sigma < 0$. σ designates the damping coefficient.

The third property demonstrated by Bland [13] is that the poles and zeros are alternate:

$$z_1 < p_1 < z_2 < p_2 < z_3 < p_3 < z_i < p_i. \tag{9}$$

One can write equation (8) in the form

$$E^*(j\omega) = A \frac{(j\omega + z_{11})}{(j\omega + p_{11})} \frac{(j\omega + z_{22})}{(j\omega + p_{22})} \cdots \frac{(j\omega + z_{nn})}{(j\omega + p_{nn})}. \tag{10}$$

In equation (10) the factors in the numerator and in the denominator are assembled two by two. Each quotient describes the behaviour of E^* in the interval $z_{ii} < \omega < p_{ii}$. The ratio $k_i = p_{ii}/z_{ii}$ determines the slope of $|E^*(\omega)|$ as well as the phase in the interval.

If the slope is weak, this ratio is slowly varying and the frequency interval is narrow. In Figure 1 is shown, in terms of the dimensionless frequency variable ω/ω_a, the quotient

$$k \frac{(j\omega + z_i)}{(j\omega + p_i)} = \frac{kz_i}{p_i} \frac{(j\omega/z_i + 1)}{(j\omega/p_i + 1)} = \frac{(j\omega/\omega_a + 1)}{(j\omega/k\omega_a + 1)}. \tag{11}$$

It can be shown [14] that the slope s of the curve of $|E^*(\omega)|$ at the inflexion point $\omega = k^{0.5}\omega_a$ is related to the ratio $k = p_i/z_i$ by

$$k = (s + 1)/(1 - s). \tag{12}$$

Consequently, equation (12) allows one to determine the frequency interval k as a function of s. Values of k are shown in Table 1.

If one takes the decimal logarithm of equation (10)

$$|E^*(\omega)|_{dB} = 20 \log_{10} A + \sum_{i=0}^{N} 20 \log_{10} (j\omega + z_{ii}) - \sum_{i=0}^{N} 20 \log_{10} (j\omega + p_{ii}),$$

$$\varphi = \sum_{i=0}^{N} \operatorname{arctg} \frac{\omega}{z_{ii}} - \sum_{i=0}^{N} \operatorname{arctg} \frac{\omega}{p_{ii}}. \tag{13}$$

The graphical construction of Bode's plot is simple, in view of equations (13). Gains in decibels as well as phases φ are additive with appropriate signs.

2.2. GRAPHICAL AND NUMERICAL EVALUATION OF POLES AND ZEROS

Consider a simple example of a harmonic test response, as follows, with $p = j\omega$:

$$E^*(p) = \frac{10(p + 50)(p + 150)(p + 500)(p + 1000)(p + 3100)}{(p + 100)(p + 200)(p + 800)(p + 1500)(p + 5000)}. \tag{14}$$

$E^*(p)$ covers four decades of frequency with five poles and zeros. This test function is directly invertible after decomposition into simple elements:

$$\begin{aligned} E(t)/10 = {} & 0{\cdot}96875 - 0{\cdot}0730945(1 - \exp(-100t)) - 0{\cdot}091346((1 - \exp(-200t)) \\ & - 0{\cdot}094752(1 - \exp(-800t)) - 0{\cdot}03658(1 - \exp(-1500t)) \\ & - 0{\cdot}5544(1 - \exp(-5000t)). \end{aligned} \tag{15}$$

Equations (14) and (15) will serve to test the validity of various inversion methods. The graphical curves $|E^*(f)|$ in the frequency domain and $E(t)$ in the time domain are shown, respectively, in Figure 2.

Consider now the evaluation of the poles and zeros of $E^*(p)$ from only the curve $|E^*(f)|$ in Figure 2(a). The various steps of calculation are presented in Figure 3.

The first step is to localize the first frequency interval including the inflexion point. From the slopes at this point, k defining the interval after equation (12) is evaluated. The first pole and zero pair, p_i, z_i, is then fixed. The upper and lower adjacent frequency intervals IIa and IIb are evaluated in a similar manner. The process is continued until the two horizontal upper and lower asymptotes are reached. The number N of poles and zeros is then determined. This graphical construction is followed by a numerical optimization

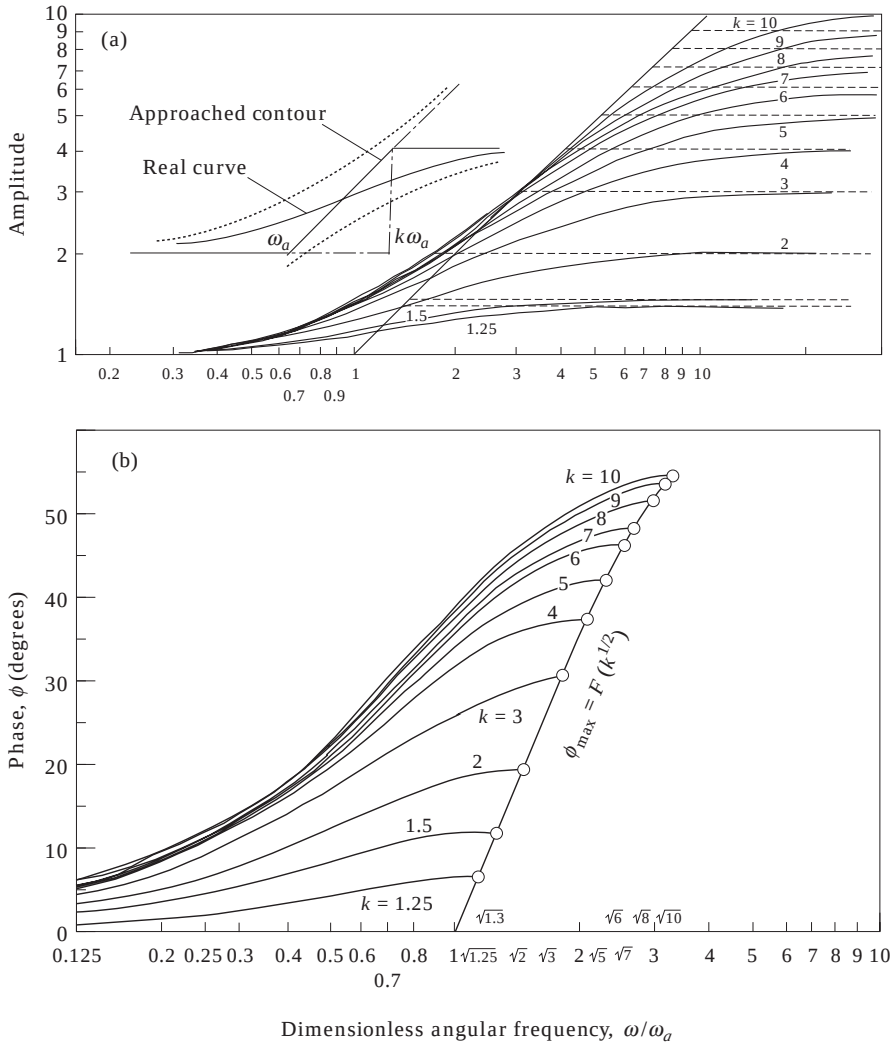

Figure 1. The amplitude and phase of the ratio $(\omega_a + j\omega)/(k\omega_a + j\omega)$ versus ω/ω_a. Curves (b) are symmetric with respect to $k^{1/2}\omega$. k is the ratio of two cut-off frequencies p/z. ϕ is the angle

$$\frac{\omega_a + j\omega}{k\omega_a + j\omega} = \text{arc tg}\,\frac{(\omega/\omega_a)(k-1)}{k + (\omega/\omega_a)^2}.$$

TABLE 1

The value of the dimensionless frequency interval k versus the slope s at the inflexion point, in Figure 1

s	*k*	*s*	*k*
0·5	3	0·38	2·2258
0·48	2·846	0·36	2·125
0·46	2·7037	0·34	2·03
0·44	2·5715	0·32	1·94
0·42	2·4482	0·3	1·857
0·4	2·333	0·25	1·666
		0·2	1·5

which improves the pole and zero localization by minimizing the quadratic errors. One obtains ten poles and ten zeros as follows, with $p = j\omega$:

$$E_a^*(p) = \frac{(p+2)(p+6{\cdot}5)(p+15)(p+32)(p+57)(p+90)}{(p+2{\cdot}3)(p+9)(p+20)(p+40)(p+65)(p+110)} \times \frac{(p+130)(p+230)(p+420)(p+960)}{(p+160)(p+270)(p+500)(p+1150)}. \tag{16}$$

Then, by decomposition into simple elements, it is easy to obtain the relaxation function by using the inverse Laplace transform:

$$E_a(t) = E_0\left[a_0 + \sum_{i=0}^{q} a_i \, \mathrm{e}^{-p'_{ii}}\right], \tag{17}$$

$$a_0 = \frac{z_1 z_2 \cdots z_n}{p_1 p_2 \cdots p_n}, \qquad a_0 = \frac{P_n(-p_{ii})}{p_n Q_{q,i}(-p_{ii})}, \qquad Q_{q,i}(-p_{ii}) = \frac{Q_p(p)}{p + p_{ii}}. \tag{18}$$

The $-p_{ii}$ are the poles of $G_a^*(p)$ in equation (16).

In Figure 4 are shown the three relaxation functions; the exact one (equation (15)), the numerically approximated function $E_a(t)$ (equation (17)), and the function $E_f(t)$ obtained by the Ninomiya–Ferry method [5]:

$$E_f(t) = E'(\omega) - 0{\cdot}4E''(\omega) + 0{\cdot}014E''(10\omega). \tag{19}$$

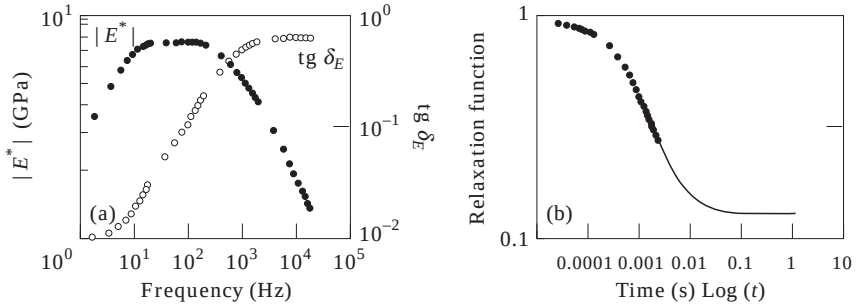

Figure 2. The test function, equation (14), used to compare various inversion methods. (a) Absolute value $|E^*|$ and damping tg δ_E; (b) relaxation function $e(t)$ obtained by direct inversion, equation (15).

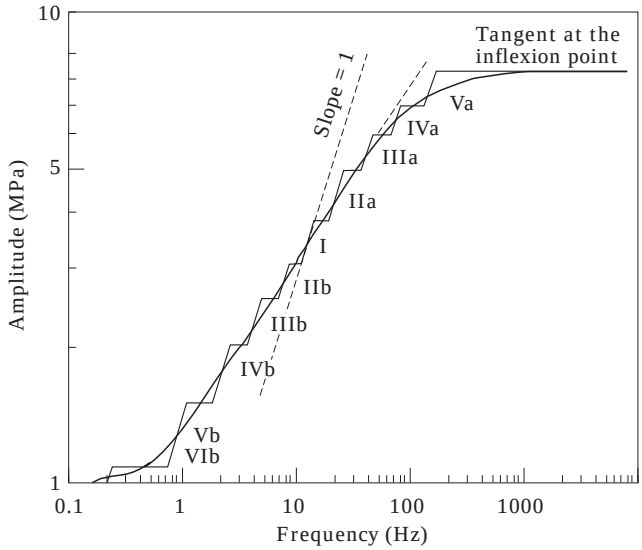

Figure 3. The determination of poles and zeros from the amplitude curve of the test function, Figure 2(a). I, IIa, IIb, IIIa, IIIb, ... designate the successive frequency intervals.

Here $t = 1/\omega$, and E' and E'' are the real and imaginary parts of the complex modulus curves deduced from the curves shown in Figures 2(a) and 2(b). The relaxation function curve produced by using equation (19) has large errors for short times, in the transition regions, and also for long times. The discrepancy between $E_a(t)$ and the exact curve $E(t)$ is small, although the poles and the zeros are different in number and in values.

2.3. FRACTIONAL DERIVATIVES

In spite of the considerable literature devoted to the application of fractional derivatives in the domain of viscoelasticity, to the authors' knowledge engineers, even in advanced industries, are not familiar with such a formulation. Consequently, it is not included in computer codes for finite element calculations. One of the reasons for this disaffection is that the inverse Fourier transform of the transfer function in terms of fractional derivatives does not use time exponential series but rather hypergeometric series. A second reason might be the direct numerical computation of fractional derivatives in the constitutive equation which is not familiar to specialists in finite elements, although it has been utilized elsewhere [8].

2.3.1. *Expression for the complex modulus*

For linear viscoelastic solids, the complex modulus versus circular frequency ω is written in its general form as

$$E^*(p) = A \prod_{i=1}^{n} [(1 + (T_i p)^{+\alpha_i}]^{\pm 1}, \tag{20}$$

with $p = \mathrm{j}\omega$. A is the static modulus, and α_i are non-integer exponents less than 1. The condition imposed on the exponents α_i is that when ω goes to infinity, the modulus $|E^*(\omega)|$ must be finite for a solid viscoelastic material.

Equation (20) can be written in an explicit form as a product of many factors:

$$E^*(p) = A\,\frac{[1+(T_1p)^{\alpha_1}]\,[1+(T_3p)^{\alpha_3}]}{[1+(T_2p)^{\alpha_2}]\,[1+(T_4p)^{\alpha_4}]}\cdots. \tag{21}$$

The condition on the α_i's implies

$$\underset{\omega\to\infty}{E^*(p)} = A\,\frac{(T_1p)^{\alpha_1}\,(T_3p)^{\alpha_3}}{(T_2p)^{\alpha_2}\,(T_4p)^{\alpha_4}}\cdots. \tag{22}$$

One must have, with $p = j\omega$,

$$\alpha_1 = \alpha_4, \qquad \alpha_2 = \alpha_3, \qquad \ldots, \tag{23}$$

and, with the classification

$$1/T_1 < 1/T_2 < 1/T_3 < 1/T_4 \ldots, \tag{24}$$

$$\underset{\omega\to\infty}{E^*}(j\omega) = A\,\frac{T_1^{\alpha_1}}{T_2^{\alpha_2}}\,\frac{T_3^{\alpha_3}}{T_4^{\alpha_4}}\cdots = A\left(\frac{T_1}{T_4}\right)^{\alpha_1}\left(\frac{T_3}{T_2}\right)^{\alpha_2}\cdots. \tag{25}$$

Conditions (23) are not satisfied in some publications [11], if the transient response is restricted to a limited time interval. That is the case for the dynamic response of mechanical structure.

Generalization of equation (21) to more than two transition zones is straightforward, by using a similar procedure.

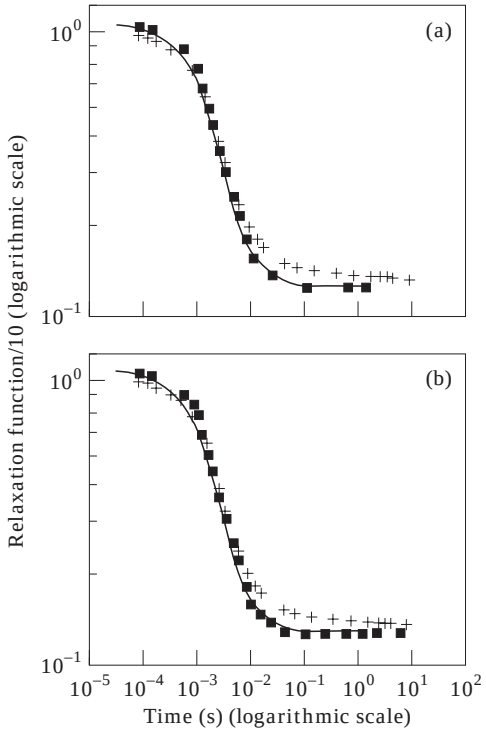

Figure 4. A comparison of various inversion methods using test function (15). (a) ——, Exact function; + + + +, Ninomiya–Ferry method [5]; ■■■■■■, present method based on polynomials. (b) ——, Exact function; ■■■■■■, present method based on fractional derivatives; + + + +, Ninomiya–Ferry method.

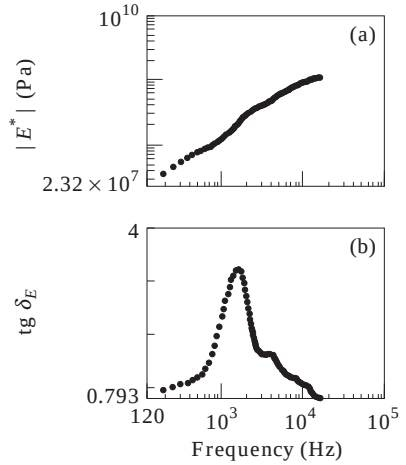

Figure 5. Young's modulus of high damping elastomer (absolute value and damping). (a) Change of slope; (b) presence of many maxima.

The presence of the product of more than one quotient in equation (21) can be explained by the microstructure of the material itself. Many polymers and elastomers are constituted of a blend of many constituents which creates, in the curve of complex modulus, many transition zones.

In Figure 5 the complex Young's modulus of a special elastomer with carbon black is presented. Clearly, the gain and phase curves present changes of slopes and many maxima, respectively.

For a great number of viscoelastic materials, the complex modulus is presented as

$$E^*(p) = A\,\frac{[1 + (T_1 p)^{\alpha_1}]}{[1 + (T_2 p)^{\alpha_1}]}. \tag{26}$$

Four coefficients, A, T_1, T_2 and α_1, are necessary to characterize such a material.

2.3.2. *Evaluation of the four coefficients of the complex modulus*

One can write equation (26) in the form

$$E^*(p) = E_0\left[1 + \frac{1}{z}\left(\frac{p}{\omega_0}\right)^{\alpha}\right]\Big/\left[1 + \left(\frac{p}{\omega_0}\right)^{\alpha}\right], \tag{27}$$

with

$$\omega_0 = 1/T_0, \qquad z^{1/\alpha}\omega_0 = 1/T_1, \qquad \alpha = \alpha_1, \qquad E_0 = A. \tag{28}$$

The parameter z is the ratio of the Young's modulus evaluate at zero frequency to that at infinite frequency:

$$z = E_0/E_g, \qquad E_g = \lim_{\omega \to \infty} |E^*(\mathrm{j}\omega)|. \tag{29}$$

The two first parameters in equation (27), E_0 and z, are easily evaluated. The two remaining parameters are the exponent α and the higher cut-off circular frequency ω_0.

In the transition zone, the maximum of the damping coefficient η_M, defined as the quotient of the imaginary part to the real part of the complex modulus [14],

$$\eta_M = \mathscr{I}m\,[E^*]/\mathscr{R}e\,[E^*], \tag{30}$$

is localized at the frequency ω corresponding to the inflexion point of the amplitude curve (absolute value),

$$\alpha = \frac{2}{\pi} \arcsin \frac{\eta_M[2(1-Z)Z^{1/2} + (1-Z)^2(1+\eta_M^2)^{1/2}}{\eta_M^2(1+Z)^2(1-Z)^2}. \tag{31}$$

In Figure 6 is shown the graphical representation of the parameters E_0, E_g and η_M which is used to evaluate α in equation (31).

The evaluation of the cut-off frequency ω_0 is effected by the Newton–Raphson method as follows.

The problem to be solved can be formulated as the minimization of quadratic errors between theoretical and experimental values of the complex modulus:

$$\text{minimize } \varepsilon^2 = \sum_{i=1}^{N} [|E^*_{exp}| - |E^*_{th}(\omega_0, \alpha)|]^2. \tag{32}$$

ω_0 is taken here as the variable. By differentiation of expression (32) with respect to ω_0, one obtains

$$g = \sum_{i=1}^{N} [|E^*_{exp}| - |E^*_{th}(\omega_0, \alpha)|] \frac{\partial |E^*_{th}(\omega_0, \alpha)|}{\partial \omega_0} = 0. \tag{33}$$

ω_0 is then evaluated by using the Newton–Raphson formula (33), which yields

$$\omega_0^{k+1} = \omega_0^k + g(\omega_0^k)/(\partial g(\omega_0^k)/\partial \omega_0^k). \tag{34}$$

The superscript k designates the kth iteration.

In section 4 the application of the method to the evaluation of the closed form expression of the complex modulus will be presented.

A flowchart, in which the successive steps of the calculation are explained, is presented in Figure 7.

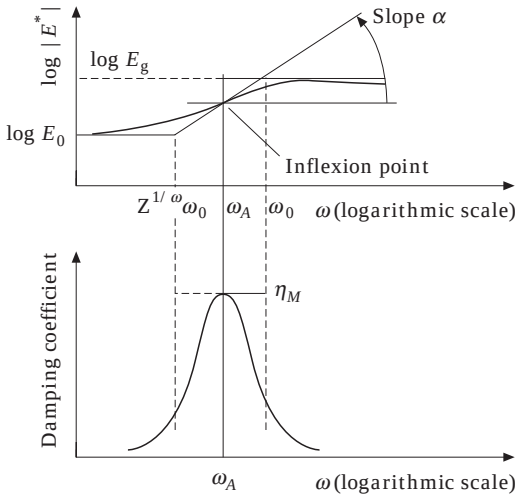

Figure 6. The exponent α evaluated from η_M, the maximum value of damping.

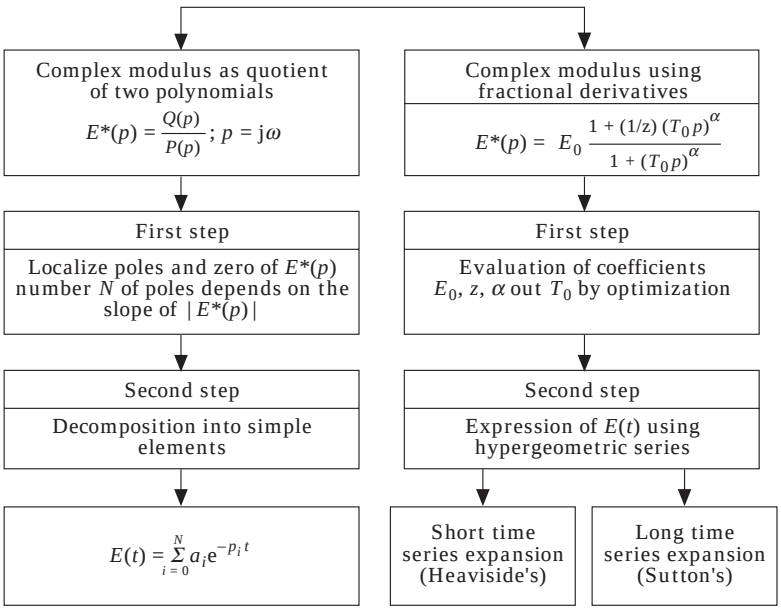

Figure 7. The two classes of methods using polynomials and fractional derivatives respectively.

3. TRANSIENT RESPONSES OBTAINED BY INVERSE FOURIER TRANSFORM

In this section, two methods of inversion are presented. The first one is relevant to the complex modulus defined in equation (10) as the quotient of two polynomials of the same order. The second method concerns the constitutive equation in terms of fractional derivatives.

The first method requires decomposition into simple elements after evaluating the poles and the zeros of the complex modulus. The inversion is straightforward. In second method a series expansion of the complex modulus is used and hypergeometric series in the time domain for the transient response. In what follows the original time function corresponding to the Carson–Laplace transform of the form $((1 + (T_1 p)^{\alpha_1})^{-1}$ is presented first. Then the inverse Laplace transform of the complex modulus in the form (26) is presented.

3.1. THE TIME FUNCTION THE CARSON TRANSFORM OF WHICH IS OF THE FORM $((1 + (T_1/p)^{\alpha_1})^{-1}$

In Appendix A details are given of the calculation of the time function

$$f(t) = \frac{1}{2\pi j} \int_{c - j\infty}^{c + j\infty} e^{tp} \frac{1}{p[1 + (T_0 p)^{\alpha}]} \, dp. \tag{35}$$

A Bromwich–Wagner contour is used with a slit from $-\infty$ to 0 on the real axis of the complex variable $p = \sigma + j\omega$, so as to obtain a holomorphic function inside the contour. The three non-zero integrals are evaluated along the real axis and around a small circle surrounding the origin; see Figure A1 of Appendix A. One thus has

$$f(t) = 1 + \frac{1}{2\pi j} \left[\int_{-\infty}^{0} \frac{e^{-\rho t} \, d\rho}{\rho[1 + (\tau\rho)^{\alpha} e^{-j\pi\alpha}]} + \int_{0}^{\infty} \frac{e^{-\rho t} \, d\rho}{\rho[1 + (\tau\rho)^{\alpha} e^{j\pi\alpha}]} \right], \tag{36}$$

with $p = \rho \exp(j\varphi)$ and $\varphi = \pm\pi$ along the real axis $\sigma < 0$. To evaluate the two integrals in equation (36) one has to expand the two denominators into series. The final result is

$$E_1(t) = E_0\left\{e^{-t/T_0}\sum_{r=0}^{\infty}(-1)^r\frac{\sin \pi r\alpha}{\pi r\alpha}\left[{}_1F_1\left(1, 1+\alpha r, \frac{t}{T_0}\right)\right.\right.$$

$$\left.\left. + {}_1F_1\left(1, 1-\alpha r-\alpha, \frac{t}{T_0}\right) - \exp\left(\frac{t}{T_0}\right)\left(\frac{T_0}{t}\right)^{\alpha r+\alpha}\Gamma(1-\alpha r-\alpha)\right]\right\}. \tag{37}$$

In equation (37) the following hypergeometric series is used [15]:

$${}_1F_1(\alpha, \beta, x) = \sum_{r=0}^{\infty}\frac{\Gamma(\alpha+r)}{\Gamma(\alpha)}\frac{\Gamma(\beta)}{\Gamma(\beta+r)}\frac{x^r}{r!}. \tag{38}$$

Γ denotes the gamma function.

Note that the hypergeometric series is the necessary mathematical companion of calculus when using fractional derivatives [16]. In the past, voluminous books devoted to numerical computations have been published with double entry tables [15]. Their utilization is cumbersome; however, things have changed. At present, convenient programs computing hypergeometric series, such as Mathematica or Jeandel Scientific, are available for computers.

3.2. INVERSION OF THE EXPRESSION FOR THE COMPLEX MODULUS

The expression to be inverted is

$$E_0\frac{[(1+(1/z)(T_0p)^{\alpha})]}{p(1+(T_0p)^{\alpha})} = \frac{1}{p[1+(T_0p)^{\alpha}]} + \frac{(1/z)(T_0p)^{\alpha}}{p[1+(T_0p)^{\alpha}]}. \tag{39}$$

Equation (39) is composed of two terms. The first one gives rise to the expression for the relaxation function in equation (37). It remains to find the original function corresponding to the second term in equation (39):

$$E_2(t) = \mathscr{L}^{-1}\left[\frac{T_0^{\alpha}}{z}p^{\alpha}E_1(p)\right] = \frac{T_0^{\alpha}}{z}\frac{1}{\Gamma(-\alpha)}\int_0^t (t-\tau)^{-\alpha-1}E_1(\tau)\,d\tau, \tag{40}$$

$$E(t) = E_1(t) + E_2(t).$$

3.3. ASYMPTOTIC EXPANSION OF TRANSIENT RESPONSE

Equations (40), (41) and (37) give a general expression for the transient response $E(t)$ in the whole range of time: short, medium and long time intervals. In practical applications, for mechanical structural transient responses, interest is focused on a short time interval. On the contrary, in rheology, the long time responses are often used: for example, the creep function. For this purpose two asymptotic series expansions are utilized.

3.3.1. *Short time response*

The Laplace transform of the transient response is

$$\frac{(1+(1/z)(T_0p)^{\alpha})}{p(1+(T_0p)^{\alpha})} = E^*(p). \tag{41}$$

The Heaviside expansion is used with the condition $|T_0 p| > 1$ to obtain the series

$$E^*(p) = \sum_{r=0}^{\infty} (-1)^r T_0^{-\alpha r-\alpha} p^{-\alpha r-\alpha-1} + \frac{1}{z} \sum_{r=0}^{\infty} (-1)^r T_0^{-\alpha r} p^{-\alpha r-1}. \tag{42}$$

This series is absolutely convergent and one can evaluate, term by term, the corresponding time response:

$$E(t) = \sum_{r=0}^{\infty} (-1)^r \left(\frac{t}{T_0}\right)^{\alpha r-\alpha} \frac{1}{\Gamma(\alpha r+\alpha+1)} + \frac{1}{z} \sum_{r=0}^{\infty} (-1)^r \left(\frac{t}{T_0}\right)^{\alpha r} \frac{1}{\Gamma(\alpha r+1)}. \tag{43}$$

3.3.2. *Long time response*

Sutton's method [17] is used here (see details in Appendix B). The expansion of expression (41) is effected with the condition $|T_0 p| < 1$:

$$E^*(p) = \sum_{r=0}^{\infty} (-1)^r (T_0 p)^{\alpha r} + \frac{1}{z} \sum_{r=0}^{\infty} (-1)^r (T_0 p)^{\alpha r+\alpha}. \tag{44}$$

Inversion term by term of the convergent series (44) gives

$$E(t) = \sum_{r=0}^{\infty} (-1)^r \frac{(T_0)^{\alpha r} t^{-\alpha r-1}}{\Gamma(-\alpha r)} + \frac{1}{z} \sum_{r=0}^{\infty} (-1)^r \frac{(T_0)^{\alpha r+\alpha} t^{-\alpha r-\alpha-1}}{\Gamma(-\alpha r-\alpha)}. \tag{45}$$

The two asymptotic expansions (43) and (45) are considered as particular cases of general formulae given in equations (38) and (40), in which the variation of time t is restricted to the interval $t/T_0 < 1$ for short time and $t/T_0 > 1$ for long time.

The two classes of methods presented above and used for inversion are summarized in Figure 7.

4. APPLICATIONS

4.1. COMPARISON OF TRANSIENT RESPONSES

With the same test function, equation (14), and using fractional derivatives one obtains the complex modulus

$$E^*(\mathrm{j}\omega) = \left[1 + \tfrac{1}{8}\left(\mathrm{j}\frac{\omega}{3800}\right)^{0{\cdot}584}\right] \Big/ \left[1 + \left(\mathrm{j}\frac{\omega}{3800}\right)^{0{\cdot}584}\right].$$

Inversions based on hypergeometric series, short time Heaviside's expansion and long time Sutton's expansion, successively give rise to the three curves presented in Figure 4(b).

The two asymptotic methods give satisfactory results in the time interval of interest. The exact hypergeometric series method gives very good results over the whole time range.

4.2. RELAXATION FUNCTIONS OF POLYAMIDE 6 (PA6)

The Young's modulus curves are shown versus frequency in Figure 8(a). From the experimental curves, the poles and zeros of the quotient of the polynomials are numerically evaluated:

$$E_p^*(p) = \frac{2864(p+250)(p+800)(p+1600)(p+2400)(p+3600)}{(p+300)(p+1000)(p+2000)(p+2600)(p+5500)} \quad \text{(GPa)}, \tag{46}$$

$$E_{fd}^*(\omega) = \frac{E_0 + E_g(\mathrm{j}\omega/\omega_0)^\alpha}{1 + (\mathrm{j}\omega/\omega_0)^\alpha}, \tag{47}$$

$$\alpha = 0{\cdot}54, \qquad \omega_0 = 4200 \text{ rad/s}, \qquad E_0 = 0{\cdot}923 \text{ GPa}, \qquad E_g = 2{\cdot}864 \text{ GPa}.$$

Subscripts p and fd refer to the polynomial method and the fractional derivative method, respectively.

In Figure 8(b) are shown three relaxation functions obtained by various methods. The Ninomiya–Ferry method gives a curve with large discrepancies compared to those of the other methods, even in the transition zone.

4.3. RELAXATION FUNCTION OF ELASTOMER

In Figure 9(a), from the experimental curve for the Young's modulus, the method of a quotient of polynomials gives the expression

$$\frac{E^*(p)}{5{\cdot}156} = \frac{(p+15)(p+42)(p+80)(p+330)(p+1800)}{(p+16{\cdot}5)(p+50)(p+100)(p+420)(p+2000)} \quad \text{(GPa)}, \tag{48}$$

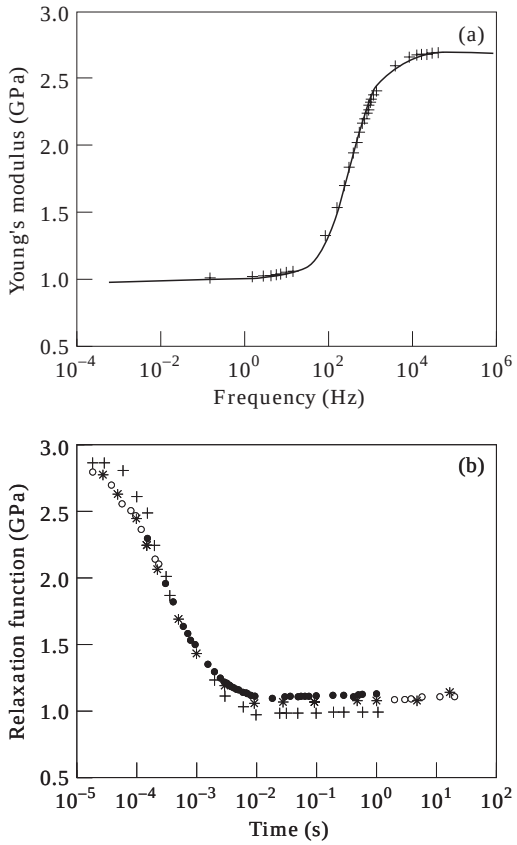

Figure 8. (a) Material polyamide 6; Young's modulus; + + + + +, experimental; ——, quotient of two polynomials. (b) Relaxation functions obtained by various methods: + + + + +, Ninomiya–Ferry; . . . . . , quotient of polynomials and exponential series; *****, fractional derivatives and hypergeometric series; ○○○○, asymptotic expansions.

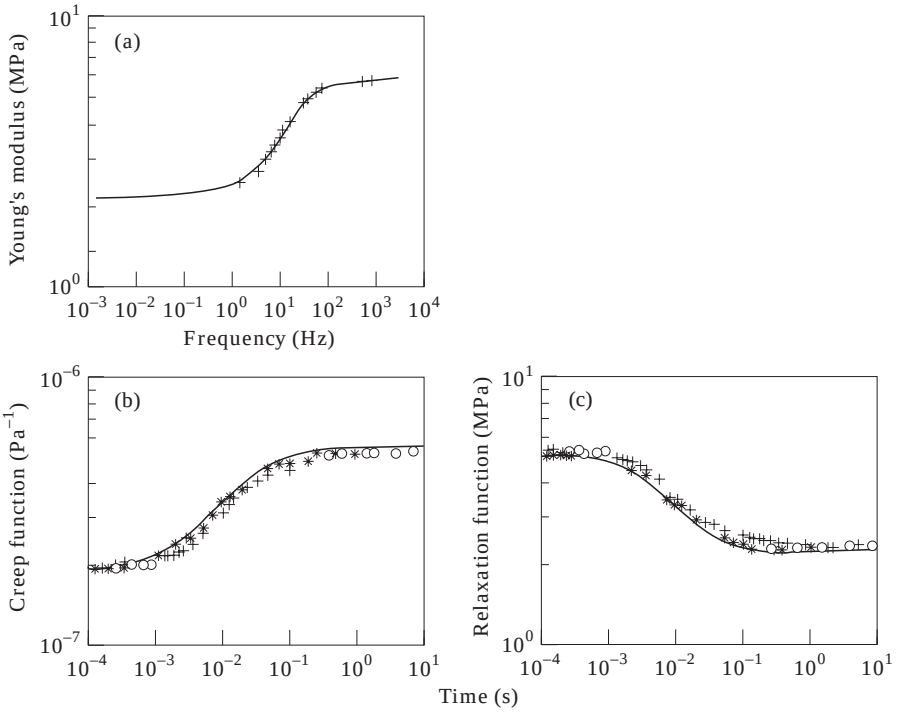

Figure 9. (a) Material elastomer; Young's modulus (absolute value); + + + + +, fractional derivatives, quotient of two polynomials. (b) Creep functions obtained by various methods: + + + + +, Ninomiya–Ferry; . . . . . , quotient of polynomials and exponential series; *****, fractional derivatives and hypergeometric series; ○○○○, asymptotic expansions. (c) Relaxation functions; key as (b).

and the functional derivative method gives the set of coefficients

$$E^*(\omega) = \frac{E_0 + E_g(\mathrm{j}\omega/\omega_0)^\alpha}{1 + (\mathrm{j}\omega/\omega_0)^\alpha}, \tag{49}$$

$$\alpha = 0{\cdot}66069, \qquad \omega_0 = 820 \text{ rad/s}, \qquad E_0 = 2{\cdot}235 \text{ MPa}, \qquad E_g = 5{\cdot}156 \text{ MPa}.$$

By using various methods of inversion, one obtains the creep (Figure 9(b)) and relaxation (Figure 9(c)) functions. Here again, the Ninomiya–Ferry method furnishes curves with large discrepancies compared to those obtained by other methods.

5. CONCLUDING REMARKS

The following remarks summarize the contributions.

The experimental complex modulus must be obtained over a large frequency range to include the static modulus E_0 and the high frequency modulus E_g.

A quotient of polynomials constitutes an efficient method to find roots and poles by appropriate numerical computations. The degree of the polynomials is not arbitrarily fixed in advance but is determined from the complex modulus curve itself. Inversion is easy.

Fractional derivatives can be used to characterize viscoelastic materials. The set of coefficients is obtained using a special optimization method.

By using hypergeometric series, transient responses are obtained over the whole frequency range. Its utilization is facilitated by the availability of special computer programs.

Two asymptotic series expansions have been presented, to obtain short time and long time transient responses, respectively.

The two classes of methods presented above do not use intermediary functions such as viscoelastic spectra which require derivatives of functions.

ACKNOWLEDGMENT

The authors gratefully acknowledge the reviewers, whose comments and remarks contributed to the improvement of the final manuscript.

REFERENCES

1. J. D. Ferry 1970 *Viscoelastic Properties of Polymers*. New York: John Wiley. Second edition. See chapters 2 and 3, pp. 59–107.
2. N. W. Tschoegl 1989 *The Theory of Linear Viscoelastic Behaviour*. New York: Springer-Verlag.
3. A. J. Staverman and F. Schwartz 1956 in *Die Physik der Hochpolymeren* (H. A. Stuart, editor). See volume IV, chapter 1. Berlin: Springer-Verlag.
4. N. P. Vinh Tuong 1967 *Memorial de l'artillerie francaise*, *vol*. *III*, 725–776. On the interrelation between harmonic and transient viscoelastic responses. (in French).
5. K. Ninomiya and J. D. Ferry 1959 *Journal of Colloid Science* **14**, 36.
6. P. E. Rouse 1953 *Journal of Chemical Physics* **21**(7). A theory of the linear viscoelastic properties of dilute solutions of coiling polymers.
7. J. D. Ferry 1970 *Viscoelastic Properties of Polymers*. New York: John Wiley. Second edition. See chapter 10, pp. 247–291.
8. J. Padovan 1987 *Computers and Structures* **27**(2), 249–257. Finite element analysis of steady and transiently moving/rolling non-linear viscoelastic structure, I: theory.
9. R. Kennedy and G. W. Padovan 1987 *Computers and Structures* **27**(2), 249–257. Finite element analysis of steady and transiently moving/rolling non-linear viscoelastic structure, II: shell and three dimensional simulations.
10. R. L. Bagley and P. J. Torvik 1986 *Journal of Rheology* **30**(1), 133–155. On the fractional calculus model of viscoelastic behavior.
11. D. R. Morgenthaler 1991 *Proceedings of Damping* **91**, 13–15 *February*, *San Diego*, *California* (edited by Wright–Patterson Laboratory, Flight Dynamics Directorate) **I**, BCA 1–BCA 28. Practical design and analysis of systems with fractional derivative materials and active controls.
12. R. F. Gibson, S. J. Hwang and C. H. Sheppard 1990 *Journal of Composite Materials* **24**, 441–451.
13. D. Bland 1960 *The Theory of Linear Viscoelasticity*. London: Pergamon Press.
14. M. Soula 1996 *Ph.D*. *Thesis*, *CNAM*, *Paris*. Etude du comportement mécanique des matériaux viscoélastiques par les dérivées fractionnaires (in French).
15. L. Slater 1960 *The Confluent Hypergeometric Function*. Cambridge: Cambridge University Press.
16. J. B. Oldham and J. Spanier 1974 *The Fractional Calculus—Theory and Application of Differentiation and Integration of Arbitrary Order*. San Diego: Academic Press.
17. H. S. Carslaw and J. C. Jaeger 1963 *Operational Methods in Applied Mathematics*. New York: Dover. See chapter 13, pp. 271–285.

APPENDIX A: INVERSION OF LAPLACE TRANSFORM $1/p[1 + (T_0p)^z]$

The Mellin–Fourier integral associated with the Bromwich–Wagner contour permits the evaluation of corresponding transient response $f(t)$ (see Figure A1):

$$f(t) = \frac{1}{2\pi \mathrm{j}} \int_{c-\mathrm{j}\infty}^{c+\mathrm{j}\infty} \mathrm{e}^{tp} \frac{1}{p[1 + (T_0p)^z]} \,\mathrm{d}p. \tag{A1}$$

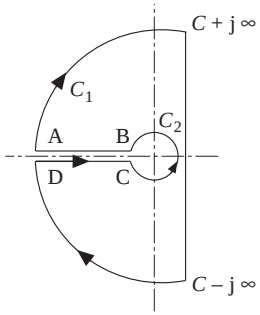

Figure A1. The Bromwich–Wagner integration contour in the complex plane $p = j\omega + \sigma$ to evaluate the relaxation function $E_r(t)$.

The function $1/p[1 + (T_0p)^\alpha]$ is multi-valued and has a critical point at the origin in the complex plane $p = \sigma + j\omega$. The contour must include a slit for negative values of σ, $-\infty < \sigma < 0$, and a small circle C_2 around the origin. The contour, with appropriate directions for each portion, is shown in Figure A1. Then the integral is decomposed into four integrals:

$$E(t) = \frac{1}{2\pi j}\left[\int_{C_1} + \int_{DC} + \int_{BA} + \int_{C_2}\right]. \tag{A2}$$

When the radius of C_1 goes to infinity, the first integral in equation (A2) tends to zero. When the radius of C_2 goes to zero, the fourth integral tends to $+1$.

The two remaining integrals in equation (A2) are

$$I_2 = \frac{1}{2\pi j} J_2 = \frac{1}{2\pi j}\int_{DC} e^{tp}\frac{1}{p(1 + (T_0p))^\alpha}\,dp, \tag{A3}$$

$$J_2 = \int_{-\infty}^{0} \frac{e^{-\rho t}\, e^{-j\pi}\, d\rho}{-\rho[1 + (\rho T_0)^\alpha\, e^{-j\alpha\pi}]} \qquad \text{with } p = \rho\, e^{-j\pi}, \tag{A4}$$

$$I_1 = \frac{1}{2\pi j} J_1 = \frac{1}{2\pi j}\int_{BA} e^{pt}\frac{1}{p(1 + (T_0p))^\alpha}\,dp,$$

$$J_1 = \int_{0}^{\infty} \frac{e^{-\rho t}\, e^{j\pi}\, d\rho}{-\rho[1 + (\rho T_0)^\alpha\, e^{j\alpha\pi}]} \qquad \text{with } p = \rho\, e^{j\pi}. \tag{A5}$$

To evaluate J_2, one has to expand the function $1/p(1 + (T_0p)^\alpha)$ into a series as follows:

$$\frac{1}{p(1 + (T_0p)^\alpha)} = \sum (-1)^r A^r u^{\alpha r - 1} \qquad \text{for } |u| < \frac{t}{T_0}, \tag{A6}$$

with $A = (T_0/t)^\alpha\, e^{-j\alpha\pi}$, and the change of variables $pt = u$, and

$$\frac{1}{p(1 + (T_0p)^\alpha)} = \sum (-1)^r A^{-r-1} u^{-\alpha r - \alpha - 1} \qquad \text{for } |u| > \frac{t}{T_0}. \tag{A7}$$

Equation (A4) is now written as the sum of three integrals:

$$J_2 = \sum_{r=0}^{\infty} \int_0^{t/T-\varepsilon} (-1)^r A^r u^{\alpha r-1} \exp(-u)\,\mathrm{d}u + \sum_{r=0}^{\infty} \int_{t/T+\epsilon}^{+\infty} (-1)^r A^{-r-1} u^{-\alpha r-\alpha-1} \exp(-u)\,\mathrm{d}u$$

$$+ \int_{t/T-\varepsilon}^{t/T+\varepsilon} \frac{\exp(-u)\,\mathrm{d}u}{u[1+Au^{\alpha}]}. \tag{A8}$$

When $\varepsilon \to 0$ the last integral tends to zero. In equation (A8) there remain two integrals. The first integral is easily identified as a confluent hypergeometric series [15]:

$$\int_0^{t/T_0} (-1)^r A^{-r-1} u^{-\alpha r-\alpha-1} \exp(-u)\,\mathrm{d}u = (-1)^r A^r \left(\frac{t}{T}\right)^{\alpha r} \mathrm{B}(\alpha r, 1)\,{}_1\mathrm{F}_1\left(\alpha r, \alpha r+1, -\frac{t}{T}\right). \tag{A9}$$

The hypergeometric series ${}_1\mathrm{F}_1(a, b, x)$ is defined in equation (38). $\mathrm{B}(x, y)$ is Euler's function,

$$\mathrm{B}(x, y) = \frac{\Gamma(x)\Gamma(y)}{\Gamma(x, y)}, \qquad x > 0, \quad y > 0. \tag{A10}$$

The second integral in equation (A8) is identified as the Kummer series [15], $\mathrm{U}(a; b; x)$:

$$\int_{t/T_0}^{+\infty} u^{-\alpha r-\alpha-1} \exp(-u)\,\mathrm{d}u = \exp\left(-\frac{t}{T_0}\right)\left(\frac{T_0}{t}\right)^{\alpha r+\alpha} \mathrm{U}\left(1, 1-\alpha r-\alpha, \frac{t}{T_0}\right), \tag{A11}$$

$$\mathrm{U}(a; b; x) = \frac{\mathrm{e}^x}{\Gamma(a)} \int_1^{+\infty} w^{a-b-1} w^{a-1} \exp(-xw)\,\mathrm{d}w. \tag{A12}$$

In equation (A11) $\mathrm{U}(a; b; x)$ is again identified as a hypergeometric series [15].

The evaluation of J_1 in equation (A5) follows a similar procedure as above.

Assembling the three integrals in equation (A2), one obtains

$$f(t) = \mathrm{e}^{-t/T_0} \sum_{r=0}^{\infty} (-1)^r \frac{\sin \pi r\alpha}{\pi r\alpha} \left[{}_1\mathrm{F}_1\left(1, 1+\alpha r, \frac{t}{T_0}\right) + {}_1\mathrm{F}_1\left(1, 1-\alpha r-\alpha, \frac{t}{T_0}\right) \right.$$

$$\left. - \exp\left(\frac{t}{T_0}\right)\left(\frac{T_0}{t}\right)^{\alpha r+\alpha} \Gamma(1-\alpha r-\alpha) \right]. \tag{A13}$$

This equation is valid over the whole range of time $0 < t < \infty$.

APPENDIX B: SUTTON'S METHOD FOR LONG TIME RESPONSE

The Laplace transform is expanded into series [17] (see Figure B1)

$$\mathscr{L}[f(t)] = \sum_{n=0}^{\infty} a_n (p-p_0)^{n-1} + (p-p_0)^{\alpha-1} \sum_{n=0}^{\infty} b_n (p-p_0)^n, \tag{B1}$$

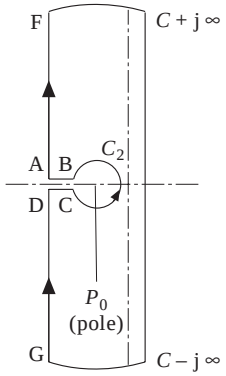

Figure B1. Sutton's contour in the complex plane $p = j\omega + \sigma$ to evaluate the relaxation function $E_r(t)$ for long time. $0 > \mathrm{Re}\, p_0 > \mathrm{Re}\, p_1 > \cdots > \mathrm{Re}\, p_n$.

with $0 < \alpha < 1$. p_0 is the singular point the real part of which is nearest to the origin. If the condition $|p - p_0| < 1$ is satisfied, $f(t)$ has an asymptotic expansion

$$f(t) \approx e^{p_0 t}\left[a_0 + \frac{\sin \pi\alpha}{\pi} \sum_{n=0}^{\infty} (-1)^n b_n \Gamma(\alpha + n) t^{-\alpha - 1}\right]. \tag{B2}$$

Concerning the transform $1/p(1 + (T_0 p)^{\alpha})$, the singular point is at the origin $p_0 = 0$. Equation (B2) consequently can be rewritten as

$$f(t) \approx \left[a_0 + \frac{\sin \pi\alpha}{\pi} \sum_{n=0}^{\infty} (-1)^n b_n \Gamma(\alpha + n) t^{-\alpha - 1}\right]. \tag{B3}$$